2015

TESTING THE EFFICIENCY OF A SERIES HYBRID DRIVETRAIN FOR AGRICULTURAL APPLICATIONS

Joseph W. Jackson
University of Kentucky, joeyjack7@gmail.com

STUDENT AGREEMENT:

I represent that my thesis or dissertation and abstract are my original work. Proper attribution has been given to all outside sources. I understand that I am solely responsible for obtaining any needed copyright permissions. I have obtained needed written permission statement(s) from the owner(s) of each third-party copyrighted matter to be included in my work, allowing electronic distribution (if such use is not permitted by the fair use doctrine) which will be submitted to UKnowledge as Additional File.

I hereby grant to The University of Kentucky and its agents the irrevocable, non-exclusive, and royalty-free license to archive and make accessible my work in whole or in part in all forms of media, now or hereafter known. I agree that the document mentioned above may be made available immediately for worldwide access unless an embargo applies.

I retain all other ownership rights to the copyright of my work. I also retain the right to use in future works (such as articles or books) all or part of my work. I understand that I am free to register the copyright to my work.

REVIEW, APPROVAL AND ACCEPTANCE

The document mentioned above has been reviewed and accepted by the student's advisor, on behalf of the advisory committee, and by the Director of Graduate Studies (DGS), on behalf of the program; we verify that this is the final, approved version of the student's thesis including all changes required by the advisory committee. The undersigned agree to abide by the statements above.

Joseph W. Jackson, Student

Dr. Joseph Dvorak, Major Professor

Dr. Donald G. Colliver, Director of Graduate Studies

TESTING THE EFFICIENCY OF A SERIES HYBRID DRIVETRAIN FOR AGRICULTURAL APPLICATIONS

THESIS

A thesis submitted in partial fulfillment of the requirements for the degree of Master of Science in Biosystems and Agricultural Engineering in the College of Engineering at the University of Kentucky

By

Joseph W. Jackson

Lexington, Kentucky

Director: Dr. Joseph Dvorak, Professor of Biosystems & Agricultural Engineering

Lexington, Kentucky

2015

ABSTRACT OF THESIS

TESTING THE EFFICIENCY OF A SERIES HYBRID DRIVETRAIN FOR AGRICULTURAL APPLICATIONS

Because of high fuel costs and rising concern over controlling motor vehicle emissions, there has been a surge in the number of hybrid passenger vehicles on roads in recent years. This transition has not yet been seen with agricultural vehicles. With this in mind, this study created a test scheme to characterize and replicate agricultural loads, and design of a hybrid drivetrain that is suitable for agricultural purposes.

Torque and power data were recorded from the controller area network of a tractor performing a baling operation. The recorded data was characterized using statistical and time series analyses, and converted into a simplified torque profile that could be run on a common type of dynamometer.

The prototype series hybrid drivetrain was subjected to the simplified profile developed, and drivetrain efficiency was compared to the efficiency under constant load. The effect of battery pack, and engine size was also tested. On average, the prototype developed was not more efficient than a similarly sized standard geared vehicle, but there is significant room for further optimization.

KEYWORDS: Tractor, Electric, Load Characterization, Hybrid Drivetrain, Dynamometer

Joseph W. Jackson

8/21/15

TESTING THE EFFICIENCY OF A SERIES HYBRID DRIVETRAIN FOR AGRICULTURAL APPLICATIONS

By

Joseph W. Jackson

Dr. Joseph Dvorak
Director of Thesis

Dr. Donald G. Colliver
Director of Graduate Studies

8/21/15

TABLE OF CONTENTS

LIST OF FIGURES

LIST OF TABLES

LIST OF EQUATIONS

LIST OF FILES

Filename	Size (bytes)
14.3.19.1.csv	206433
14.3.19.2.csv	220081
14.3.20.1.csv	229625
14.3.20.2.csv	234619
14.4.16.1.csv	224918
14.4.16.2.csv	248858
14.4.17.1.csv	289671
14.4.17.2.csv	234416
14.4.17.3.csv	217041
14.4.18.1.csv	232050
14.4.18.2.csv	201760
14.4.18.3.csv	213643
14.4.21.1.csv	248064
14.4.21.2.csv	235483
14.4.21.3.csv	210098
14.4.22.1.csv	3162356
14.4.22.2.csv	235483
14.4.22.3.csv	193312
14.4.22.4.csv	211818
addTopXAxis.m	6019
append_pdfs.m	2061
autorunstuff.m	415
balefrequency.m	2720
boxplotgraphs.m	1375
cline.m	996
dataprocessing.m	7899
DataSummary.csv	1444
doubleaxisplot.m	0

eps2pdf.m	5149
export_fig.m	30967
fft_stats_and_plots.m	2071
fix_lines.m	5956
ghostscript.m	5169
histogramplot.m	498
im2gif.m	7300
isolate_axes.m	3794
lopper.m	137
mercator.m	3018
pdf2eps.m	1525
pdftops.m	3188
plotcolorline.m	831
PreData.csv	2907
print2array.m	6474
print2eps.m	9490
runcccstuff.m	1176
Rundata.csv	964
runthings.m	930
torquepoints2.mat	1331955
user_string.m	2462
using_hg2.m	376

CHAPTER 1: INTRODUCTION AND LITERATURE REVIEW

1.1 Introduction

1.1.1 Introduction

There has been a surge in the number of hybrid passenger vehicles on roads in recent years. This transition has not yet been seen with agricultural vehicles. Generator systems, although relatively uncommon, have been implemented on tractors before. In 1954 IH marketed a tractor with the IH ElectrAll system for on-board AC power. More recently, John Deere released their EPremium tractor series tractors. In these systems, however, the electrical power was not incorporated into the drivetrain of the tractor and was instead used to run auxiliary implements.

The main advantage of a hybrid drive system is that it has the ability to store energy during periods of low demand. This stored energy can then be used during periods of high demand. In theory, this will improve fuel efficiency because energy that would have been wasted is now being stored and utilized later. Furthermore, because electric motors can be used to generate electricity when overdriven, energy can be recovered from braking or descending inclines as well. This regenerative braking might not be applicable in fieldwork, but could be useful during bulk material transportation tasks. Hybrid-electric drivetrains on tractors have the potential for fuel savings, but the feasibility must be evaluated.

1.1.2 Project objectives

The main goals of this research are to discover the feasibility of hybrid drivetrains as a method of reducing fuel consumption for agricultural vehicles, and how a hybrid drivetrain responds to agricultural loading. In order to accomplish these objectives, the study was divided into two sections:

1. Objective one is to develop a strategy for running repeatable tests that accurately represent typical agricultural loading. This includes:
    - Recording pertinent data from a tractor during a field operation.
    - Characterizing the recorded data, and transforming it into a form that can be run on a dynamometer.
2. Objective two is to design and test a hybrid drivetrain. This includes:

- Subjecting a hybrid drivetrain to the representative agricultural load pattern found upon completion of objective one.
- Monitoring power and efficiency of components throughout the hybrid system.

1.2 Literature Review

1.2.1 Agricultural Load Characterization

Fuel costs are a significant factor in many agricultural machinery operations so considerable research has been performed to improve fuel efficiency. In 2010, farm diesel use was 5.4% of the total United States diesel use, and 65% of that farm diesel use was in crop production (Hoy et al., 2014). The design of the powertrain is one of the most important factors in determining fuel efficiency. One of the first steps in any powertrain design is to consider the loads to which the powertrain will be subjected. These loads have traditionally been presented as averages as in ASABE Standard D497.7 (American Society of Agricultural and Biological Engineers, 2011) but the variations in loading over time have a significant impact on fuel efficiency and even exhaust emissions (Hansson, Lindgren, Nordin, & Pettersson, 2003). Variations are even more important for hybrid powertrains which are generally used because of their efficiency in handling variable loads (Myong-Jin et al., 2012). Although variations in loads are important in powertrain design, Hansson et al. (2003) point out that there had been no attempts to measure variability in agricultural loads on powertrains prior to their study in 2003.

Careful analysis of power requirements and their distribution is also necessary to permit the development of fleets of small agricultural vehicles as envisioned by Blackmore, Have, and Fountas (2002), Emmi, Paredes-Madrid, Ribeiro, Pajares, and Gonzalez-de-Santos (2013), Pitla, Luck, and Shearer (2010) and others. Blackmore et al. (2002) states that current technology implies that these machines need internal combustion engines for energy density. Improvements in other forms of energy storage could enable even smaller machines without internal combustion engines. Identifying when energy densities provided by new technologies has reached the point where structures not based on internal combustion engines become feasible will require detailed information on the expected power output from these machines. This information must

come from analyzing and characterizing the time-varying load levels the machines would experience while performing their expected tasks. These machines will be unusable if they are consistently unable to complete their routes because they run out of fuel, and new forms of energy storage are likely to be initially expensive so careful optimization will be needed. Understanding the expected operational power requirements and information on how a vehicle's powertrain will respond to those requirements allow a route planner to efficiently map vehicle routes to ensure they do not run out of fuel or waste extra time refilling.

Previous researchers have investigated the variable forces imposed on agricultural equipment during operations – even if they were not focused on powertrain design. Rahama and Chancellor (1994) performed a statistical and frequency analysis of forces during plowing to improve axle and frame design better handle fatigue. This type of analysis proved useful for characterizing the loading on the tractor in a concise manner with minimal loss of information.

Hansson et al. (2003) measured the time varying loads during four different agricultural operations that had been selected to generate different levels of variability. They were able to demonstrate a decrease in fuel efficiency of 13.1% in the most variable operations, but they do not attempt to analyze or quantify the load variability. The later studies by (Myong-Jin et al., 2013) do present an analysis of load variability, but they focus on features at frequencies between 1 and 100 Hz. Their study was intended to assist in the development of a parallel hybrid powertrain. This frequency range (1 to 100 Hz) is important for engine design or for parallel hybrid transmission design as these components must respond very quickly. However, agricultural loads also produce lower frequency variations as vehicles enter or exit headlands or encounter field and crop condition changes.

While analyzing expected loads and load variation is an important part of machinery design in general, it is especially essential to designing a hybrid system. A proper model of the expected loading is needed to properly size the electric drive components and ensure there is sufficient energy storage capacity to supply power during variations in load and recover in a reasonable amount of time.

1.2.2 Drivetrain testing

In the United States, the Environmental Protection Agency regulates and tests the fuel efficiency of passenger automobiles. Tractors, on the other hand, are tested according to the Organization for Economic Co-operation and Development (OECD) codes to verify manufacturer claims on horsepower, maximum towing capacity, and other performance data. In the United States, this testing is often done at the Nebraska Tractor Test Laboratory (NTTL).

Power testing of tractors is performed at steady state conditions. The engine speed is held constant while the tractor is geared to operate within a certain speed range under load. During this testing fuel consumption is monitored, but the results of the test do not necessarily accurately represent the fuel consumption for field operations.

The loading pattern that the average agricultural tractor must handle is highly diverse; ranging from steady loads to highly variable ones, as well as from primarily PTO power to draft towing. In general, load conditions on a tractor vary in response to several factors. Terrain type affects loading, as do soil conditions. Crop density also has an effect on load level. Often farmers strive to reduce variation in crop density within a field; however, weeds and soil quality can still result in uneven crop volume.

A 1985 survey of Kansas corn farmers of fuel consumed and area covered for various field operations illustrates the effect that operation type has on fuel consumption rate (Schrock, Kramer, & Clark, 1985). Plowing the fields with a moldboard plow resulted in a mean fuel consumption per hectare of over twice that of disking, and over eight times as much as spreading fertilizer. The study does not indicate fuel efficiency, because work done was not measured. It does, however demonstrate the range of power levels to which a tractor is subjected even among the operations involved with one type of farming.

Coffman, Kocher, Adamchuk, Hoy, and Blankenship (2010) tested tractor fuel consumption under variable load by subjecting a tractor at constant speed to varying torque loads. The operating range of 50% to 90% of full drawbar torque was divided uniformly into 2.5% increments, and an equal amount of time was spent at each load level. A later study done by Howard, Kocher, Hoy, and Blankenship (2013) utilized a reduced number of load levels – six load levels in 10% increments between 30% and

80%, but added different travel speeds as well. Fuel consumption of tractors is generally observed at steady state conditions, but the load conditions to which a tractor is subjected are often variable in nature. Transient load properties have an effect on the fuel efficiency of a tractor compared to steady-state, and load variation reduces the fuel efficiency compared to the efficiency under steady-state loading for the same power consumption (Hansson et al., 2003).

Different tractor operations have different power consumption characteristics. Hansen, Walker, Lyne, and Meiring (1986) collected power consumption data for several tillage related operations in the form of power map surfaces. The machinery operator can also affect fuel efficiency because of variation in driving habits. Low field speed had lower fuel consumption per second, but took proportionately more time. Average fuel consumption was similar between varied field speed levels done at the same engine speed. The gearing of the tractor did not have an effect on the specific fuel consumption. The fuel consumption per acre was dependent on the engine speed, not the field speed.

1.2.3 Electric drivetrains in agriculture

Research on electric drivetrains in agriculture is mostly relegated to battery powered electric vehicles. Based on a model developed by Alcock (1983), utilizing lead-acid batteries as primary fuel storage for agricultural vehicles was possible, but was impractical for most agricultural activities. The most feasible use of battery-only power was for light-duty work.

The power to weight ratio of a battery powered tractor is a limiting factor. The larger a battery that is used, the more power is required to move the weight of the battery (N.L. Buck, 1983). In order to have enough power to perform basic agricultural tasks, the battery pack becomes prohibitively heavy. N.L. Buck (1983) determined that most of the power consumed in a battery powered tractor in transportation or hauling tasks would be used to move its own weight. Current deep cycle battery technologies have increased energy density compared to the estimates made in 1983. A battery pack with the same capacity as the 7.5 Mg pack estimated in N.L. Buck (1983) weighs 6.1 Mg using modern lead-acid deep cycle batteries. However, this improvement is not enough to make battery powered tractors feasible.

Modern hybrid and electric vehicles make use of other battery chemistries like Nickel metal hydride (NiMH) and Lithium-ion (Li-ion) batteries. While these battery chemistries have up to three times the energy density of lead acid batteries (Pollet, Staffell, & Shang, 2012), there are additional concerns such as costs and safety. Agricultural vehicles are operated in rough terrain and dirty conditions. The risk of damage to the batteries under normal operation is higher than in on-road vehicles.

The capabilities of battery powered agricultural equipment that use lead-acid batteries are improved somewhat by adding solar panels. Solar panels are not sufficient to supply the full required power of a tractor, but can extend the working range of the electric vehicle (Mousazadeh et al., 2010). Mousazadeh et al. (2010) found that solar panels covering the entire footprint of the tractor were able to supply about 18% of the energy used during operation. Even with the solar panels and a 700 kg 16.5 kWh battery pack, the operating time for plowing was only 4 hours. This length of operation is too short for the scale of most farming operations. In order to charge the batteries for a 4 hr operating time using only solar power, a 26 m^2 array of solar panels would be necessary.

Despite the limitations of battery power, electromechanical equipment in agriculture can still be beneficial. Electric motor control advances – specifically the advent of isolated gate bipolar transistors since the late 1980s – have allowed for better control of electric systems as they have developed over the years. These improvements have opened the door for the implementation of electric drives on agricultural equipment. (Kenneth, Joachim, Bin, & Edwin, 2013)

A vehicle with an electric drivetrain has the advantage of very rapid response to torque demands, motors can be attached to individual wheels for four-wheel traction control, and torque and power consumption can be monitored easily and accurately (Hori, 2004). These benefits are especially valuable in the off-road conditions commonly seen in agriculture. Another advantage to onboard electrical power is the ability to use electrically driven implements. Using electrically driven implements allows for better implement control, as well as enabling implement redesigns and improvements. (Buning, 2010)

1.2.4 Hybrid systems

The hybrid drivetrain configuration discussed in this thesis is a series hybrid drivetrain. Series hybrid drivetrains are those in which the full power of an internal combustion engine is converted to electrical energy which is then used to drive electric wheel motors. This is in contrast to parallel hybrid systems that are commonly used in automotive hybrid vehicles. Parallel hybrids are ones in which the power from an electric generator/motor is coupled in parallel with a mechanical transmission. In these hybrids, there is a mechanical connection between the engine to the wheels, and an electric motor/generator is used to add or remove a percent of the energy from the drivetrain. Series hybrids are simpler to design, but lose some of their advantages relative to parallel hybrids when transitions from full forward to full reverse are infrequent or not required (Karner, Prankl, & Kogler, 2012).

A key strength of hybrid systems is that the engine can be sized for the average load and energy storage can be used to compensate for occasional higher or lower loads. Utilizing this strength, however, requires an understanding of low frequency variations as they affect when and how much energy is stored or released. Also, as presented by many researchers, fuel consumption and efficiency in diesel engines vary with engine speed and torque load (Goering & Cho, 1988; Hansson et al., 2003; Harris, 1992; Harris & Pearce, 1990) so even low frequency variations will have an effect on overall fuel efficiency.

The series hybrid drivetrain is able to decouple engine speed from ground speed because the engine is no longer mechanically connected to the wheels. Coupled with the ability to store energy under periods of low load, the engine can be operated in the most efficient rpm range throughout the fieldwork regardless of field speed.

CHAPTER 2:LOAD RECORDING AND TEST DESIGN

2.1 Introduction

The goal of this chapter is to develop a method of drivetrain testing that simulates field conditions using a dynamometer. To obtain repeatability as well as variability, it is necessary to utilize a dynamometer. A dynamometer allows loads to be applied in a

consistent manner between each repeated test run. The resistance applied by the dynamometer can be varied to adjust the loading throughout the duration of the test. By dynamically changing the torque load applied to the tractor, field conditions can be simulated in a consistent manner.

In order to make the test methods more widely applicable, the profile is developed for use on a water brake dynamometer. This type of dynamometer is relatively inexpensive, and commonly used for power testing. Despite their ubiquity, water brake dynamometers are not designed for rapidly fluctuating load patterns, so some resolution was sacrificed in order to make the load profile simple enough to be compatible with a water brake dynamometer. To make the analysis used throughout this work scalable to different sized engines and drivetrains, torque values are presented as the percent of full torque of the motor or drivetrain.

Simulating field conditions involves first recording the power consumption and torque load data from a tractor performing field operations. The data must be interpreted to determine the pertinent characteristics of fieldwork. This will establish the nature of loading to which a tractor is subjected under normal use, and the interpreted data can be used to develop representative load profiles. The hybrid drivetrain can then be subjected to these representative load profiles.

2.2 Materials and Methods

2.2.1 Field Operation Description

Replicating realistic agricultural loads onto a test drivetrain requires determining the operating conditions during common agricultural production operations. To discover these conditions, recordings were taken of controller area network (CAN) messages of a machine used in normal agricultural practices of a commercial (non-research) farm. The scope of this study was limited to a single field operation. The methods outlined in this thesis can also be applied to CAN recordings of other operations as a part of future work, but limiting the scope of this individual project was necessary to permit in-depth analysis of the operation.

The CAN messages were recorded from a New Holland TG305 tractor during a corn stover baling operation on a farm in western Kentucky (Logan County, Kentucky).

This operation occurred in August 2012 and lasted approximately 4600 seconds (~77 minutes). It covered portions of a 93 Ha corn field. The baler used was a New Holland BB9080 square baler which produces bales that are 0.9 m x 1.2 m x 2.4 m. At rated PTO rotational speed, the square baler is designed to actuate the plunger in the bale chamber 40 times per minute. A large square baler like the one used has a flywheel that dampens higher frequency loads and reduces the stress on the engine caused by the plunger.

The operation of baling is of particular interest, as it is a common operation for small to moderate sized tractors. It generally exhibits a mix of load levels as the load varies with crop density and accumulation of crop in the bale chamber. In addition to the expected minute to minute variations in power requirements, there is also considerable uncertainty in the time-averaged power requirements. The ASABE standard, D497.7, for implement power requirements (American Society of Agricultural and Biological Engineers, 2011) provides ranges of ±35% to ±50% depending on the type of baler used. Because of the expected variations in power requirements, this baling operation provided an excellent situation for this study.

2.2.2 Recording data during field operation

The data recorded during the experiment included the speed and position (determined by GNSS) of the tractor, percent of maximum torque load on the engine (Figure 2.1), percent of maximum engine power, engine speed, PTO speed, and engine fuel usage rate. These values were recorded at a frequency of 1 Hz.

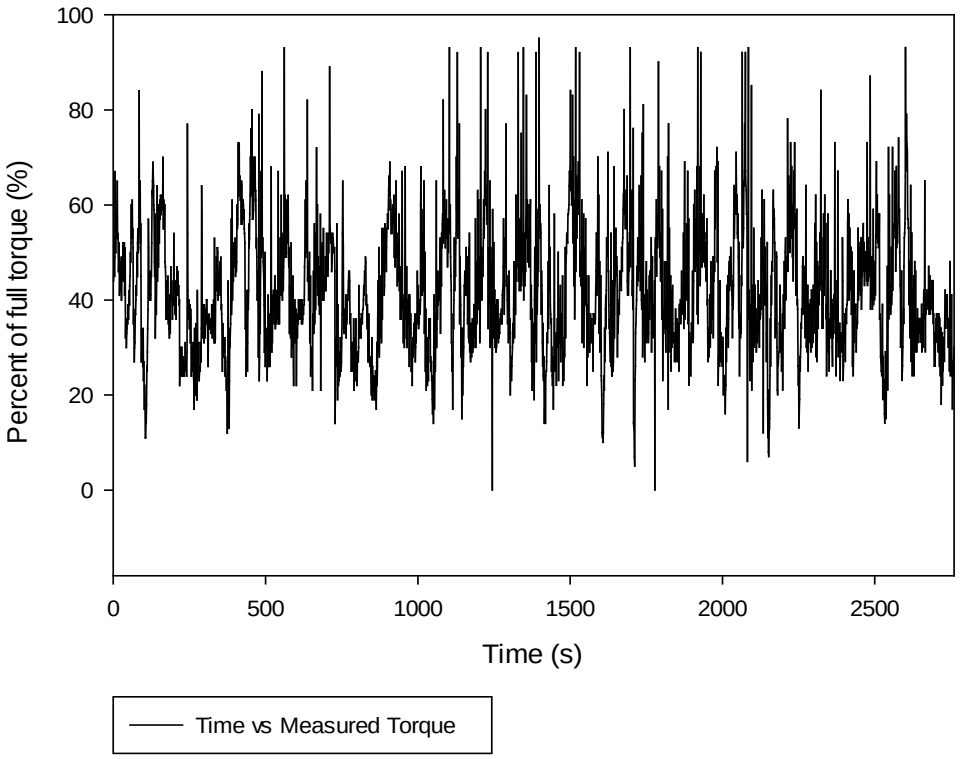

Figure 2.1 Example of information recorded from the tractor's CAN bus. This is percent of maximum available engine torque while baling.

2.2.3 Lab equipment to simulate agricultural loads

For controlled testing of drivetrains, the recorded field loads were recreated using a dynamometer in the laboratory. It was necessary to employ a dynamometer rather than actual field operations for this testing to ensure load conditions were appropriately replicated while testing different drivetrain configurations. The dynamometer used was a 33 cm DYNOmite Water-Brake Absorber (Land & Sea, Concord, New Hampshire). It is capable of producing torque loads up to 1200 N m at 3000 rpm. The torque load placed on the drivetrain was controlled by adjusting the water flow through the absorber using a manually operated valve. The water brake specifications provided a response time for a 90% output change of less than 0.5 seconds, but water intake and discharge from the dynamometer limited such 90% load changes to the several second range in actual testing.

The limitations to the dynamometer's rate of change are due to the fact that it was originally intended to measure the power of highway vehicles. As such, it is designed to operate at input shaft speeds of around 3000 rpm. The upper limit on rotational velocity for the equipment to be tested in this project was 150 rpm. A speed increaser frame was built to adjust for this, but the number of gear increases was limited to decrease the amount of losses between the drivetrain and measurement at the dynamometer. The speed increaser increased the speed to 1800 rpm. This increased speed was within the operating range of the dynamometer, but still too slow to achieve rapid load changes.

The wheels on the drivetrain to be tested were replaced with 45 tooth sprockets and coupled to a pair of 22 tooth sprockets on a connecting shaft for the initial speed increase. The shaft was connected to the input of a 1:6 gearbox. The output of the gearbox was connected directly to the input of the dynamometer. Each of the two stages of roller chains were each approximately 98% to 99% efficient (Lodge & Burgess, 2002). There was also a 1:6 ratio gearbox that is estimated at 96% to 98% efficient.

Figure 2.2 Dynamometer (foreground) attached to speed increaser frame and drivetrain to be tested.

The rotational speed of the dynamometer was measured by a Hall Effect transducer and instrumented through the data acquisition board and software that were included with the dynamometer. This speed was recorded at 1 Hz for the duration of each test run. The torque load generated by the dynamometer was recorded by a SSM-AJ-500 force transducer (Interface, Scottsdale, Arizona) which was attached to a torque arm 22.9 cm from the center of the dynamometer.

The load cell was connected by an INA126 instrumentation amplifier (Texas Instruments, Dallas, TX). The load cell was calibrated by hanging multiple weights up to 90 kg at a distance of 45.8 cm from the center of the dynamometer. The gain of the amplifier was adjusted using a potentiometer so that 404 N m corresponded with the maximum voltage and the voltage scaled linearly until there was no torque on the dynamometer.

The output of the amplifier was connected to a National Instruments USB-6259 data acquisition (DAQ) board. This DAQ board was used to record the data throughout the project. LabView (National Instruments, Austin, TX) was used to manage this data acquisition. The torque was recorded at 100 Hz and averaged over one second to produce the value for that second. The torque value was displayed on a screen updated twice per second for the person operating the water flow valve.

2.3 Results and Discussion

2.3.1 Spatial distribution of power requirements in a baling operation

Figure 2.3 illustrates the spatial distribution of torque loads while baling large square bales in a portion of a 93 Ha corn field located in Logan County, Ky. The baling operation began in the lower right corner (17.39 E,-303 N) of the map after entering the field and ended in the lower left corner (-84.93 E, -282.8 N). The map shows the path of the vehicle in addition to the torque requirements at a particular location. Clearly, there are significant variations in required torque. During turning in the headlands, a pattern of lower torque requirements in the 20-30% range is apparent. However, these levels are not among the lowest recorded as torque loads in the 5-10% range appear at various locations in straight row regions. Other than in the headlands, spatial patterns are limited as stretches of high or low torque loading occur at different locations in the field, last for different lengths of travel and can appear as sudden changes from nearby torque loads or gradual variations.

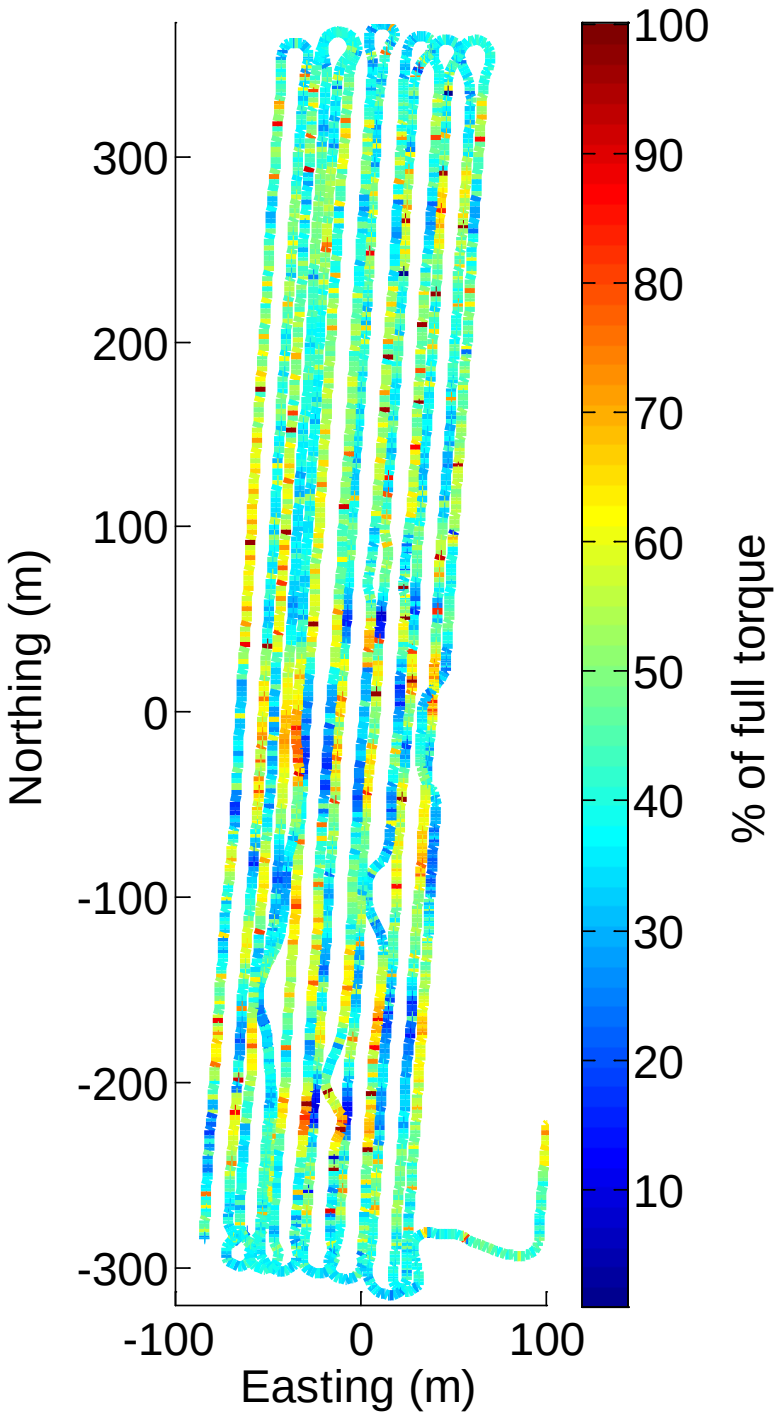

Figure 2.3 Variation in percent of full torque required as the tractor moves around the field.

2.3.2 Load Characterization

The recorded CAN messages included several pieces of operational data, but the data of primary interest for simulating agricultural loads in the lab was the required torque; as that is the variable a dynamometer can control. The torque loading pattern was characterized using two different methods, statistical analysis and time series analysis.

2.3.2.1 Statistical analysis

For statistical analysis, each data point from the torque load recorded at 1 Hz intervals was treated as an individual sample. The primary statistical characteristics of the recorded torque requirements are summarized in Table 2.1. The mean, median and mode are all tightly grouped and within 5 points of each other. The entire second quartile of torque values is highly concentrated and only stretches across 7 percentage points, from 33% to 40%. The remaining quartiles are less concentrated.

Table 2.1 Statistical characteristics of recorded torque data.

Mean Load (%)	42
Minimum Load while operating (%)	5
Maximum Load (%)	95
First Quartile Load (%)	33
Median Load (%)	40
Third Quartile Load (%)	50
Mode Load (%)	37
Standard Deviation	13

The distribution of the recorded torque requirements approximately followed a bell shaped curve (Figure 2.4) and covered nearly the entire range possible, from 5% to 95%. However, although bell shaped, it is not strictly normally distributed. Applying the one-sample Kolmogorov-Smirnov test for normality revealed that the recorded values for torque loads are not from a normal distribution. The test was performed with the null hypothesis that the data is normally distributed, against the alternative hypothesis that the data are not normally distributed at a significance level of $\alpha = 0.05$. The p-value found from the analysis was less than 0.001, so we reject the null hypothesis and conclude that the data are not normally distributed. As Figure 2.4 illustrates, there were a higher

concentration of torque loads just below the mean value in the second quartile and more values in the 90-95% range than would be expected with a normal distribution.

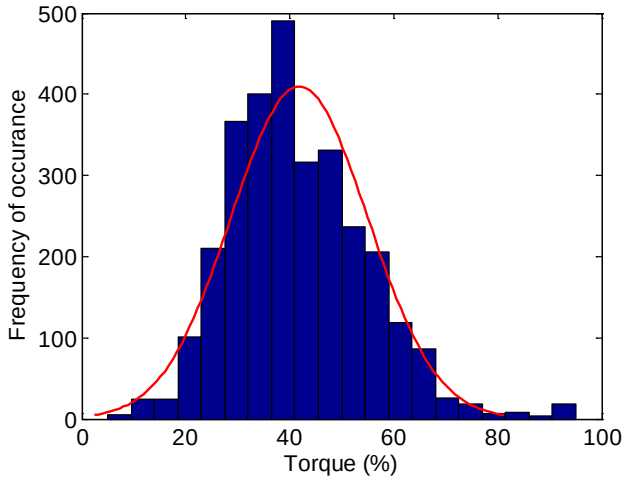

Figure 2.4 Histogram of torque requirements during a baling operation (blue) with the corresponding normal distribution (same mean and standard deviation) superimposed (red)

In general, the values below the mean were more clustered while those above the mean were more disperse. This distribution revealed that the torque requirements for a baling operation vary widely during the course of the operation. The required torque appears to frequently be in a range just below the mean but there are also a large number of occurrences when the torque requirements were significantly greater. This type of torque distribution would indicate the preference for a torque/power creation and distribution system that was capable of operating very efficiently in one range but that could also effectively scale across a wide range of values including those more than twice the base range. Further testing and data collection during other baling operations with different feedstocks, at different times of the year, and in different locations will be necessary to determine if this type of distribution is consistent for most baling operations.

2.3.2.2 Time series analysis

In the time series analysis, the torque data from the CAN messages was treated as a discrete time series with a 1 second sampling rate.

Figure 2.5 is the periodogram of the torque requirements that resulted from a Fourier transform of the time series. There are a few interesting details to note in the

data. Since the CAN data were recorded at 1 Hz, the periodogram cannot be used for frequencies higher than 0.5 Hz. The periodogram produced from the entire operation is shown in Figure 2.5; however, in this graph, it is difficult to see features at low frequencies/longer periods so figure 2.5, 2.6, and 2.7 were created which only show periods longer than 10 seonds, 20 seconds, and 50 seconds respectively. One prominent spike in torque appears at 0.3 Hz. For the baler used, the frequency of the plunger strike was 0.67 Hz. This spike at 0.3 Hz was likely caused by aliasing of the baler plunger signal due to the sampling frequency being slower than that of the plunger. Other lower amplitude spikes appear at 0.4 Hz, 0.2 Hz and at 0.1 Hz. The reasons for these spikes were less clear, but the period for these patterns would be 2.5, 5 and 10 s which would seem to indicate that they resulted from some feature of machinery operation as opposed to field structure. Field structure patterns like entering the headlands would appear at much lower frequencies. There were no sharp spikes in frequency in the 0 to 0.1 Hz (period in the 0 to 10 second) range like the one at 0.3 Hz. Regions of frequencies with higher amplitude do appear in a range of frequencies around 0.03 Hz (33 s period) and around 0.01 (100 s period).

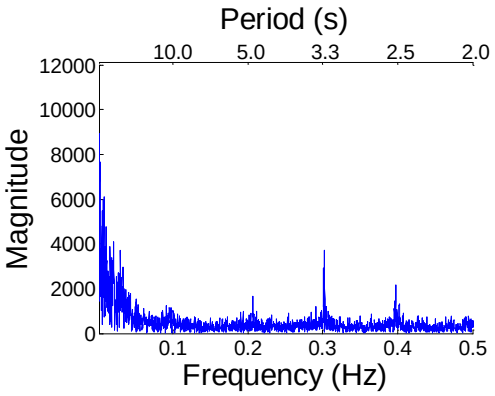

Figure 2.5 Fourier transform of data recording.

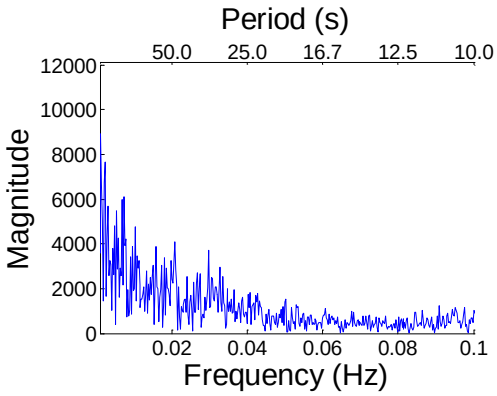

Figure 2.6 Periodogram focused on periods longer than 10 seconds.

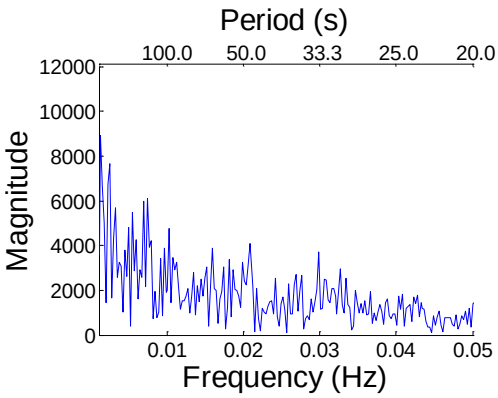

Figure 2.7 Periodogram focused on periods longer than 20 seconds.

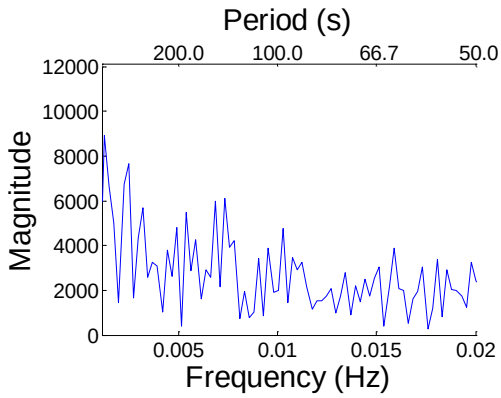

Figure 2.8 Periodogram focused on periods longer than 50 seconds.

To find reasons for other peaks in the periodogram, an analysis was conducted of several other actions that repeated during the operation. Entering and exiting the headlands of the field is a very regular event, and the vehicle entered the headlands at a frequency of 0.00366 Hz (approximately once every 273 seconds). However, although this is a regular event and the torque loads in the headlands (Figure 2.3) appear different than in other field areas, the headlands do not register as a peak on the periodogram.

Another possible source of loading effect is bale production. Within the recorded data was the timestamp for when a bale left the chamber. The histogram (Figure 2.9) shows the frequency of bale drops. Figure 2.10 marks the mean bale drop frequency, 0.00312 Hz (approximately once every 320 seconds) which corresponds to a peak on the periodogram. However, although a peak is present in the periodogram, it is not a strong peak, and it is not clear that it was only related to bale drop frequency. Other than the strong spikes in the periodogram from the baler plunger, it was difficult to ascribe any other feature in the periodogram to a specific machine or field feature without more in-depth testing.

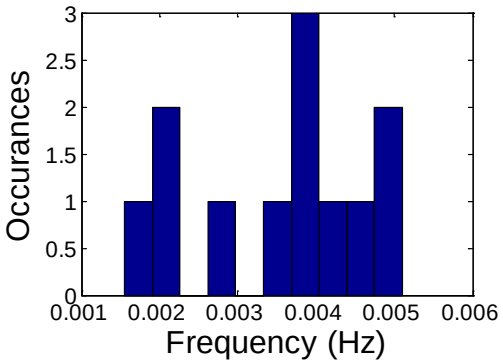

Figure 2.9 Histogram of bale drop frequency.

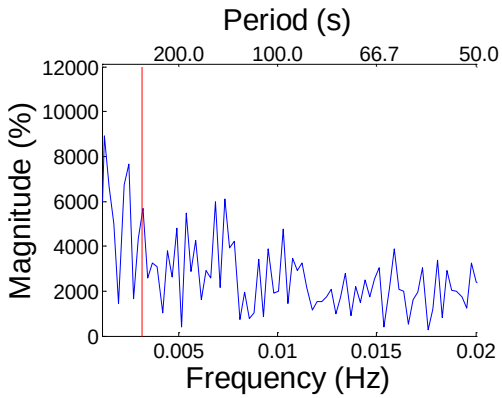

Figure 2.10 Average frequency of bale counter indexing (red) marked on a periodogram of torque requirements (blue).

2.3.3 Load recording simplification

The load data from the CAN recording was taken once every second. As seen in Figure 2.1, the load varies relatively quickly. The dynamometer was not able to respond rapidly enough to directly follow the recorded load data. A load simplification was therefore necessary. The torque load profile was down-sampled to one minute intervals by taking the value for the first second of each minute. This amount of downsampling was necessary to allow the dynamometer to reach and hold the assigned value for a sufficient amount of time that the held value contributes more to the signal than the transient portions. The value was held constant for one minute for each loading value to create the simplified loading profile shown in Figure 2.11. Decimation was also considered to create a simplified loading profile. Decimation involves filtering the data with a low pass filter prior to downsampling in order to decrease the possibility of aliasing. The cross-correlation coefficient (CCC) value was slightly higher for the decimated signal than for the downsampled signal, however the resulting profile did not match the statistical characteristics as closely as simply downsampling (Table 2.2). The decimation simplification method was ultimately rejected, as it artificially suppressed the variation inherent in the original signal, resulting in a signal with a much smaller standard deviation.

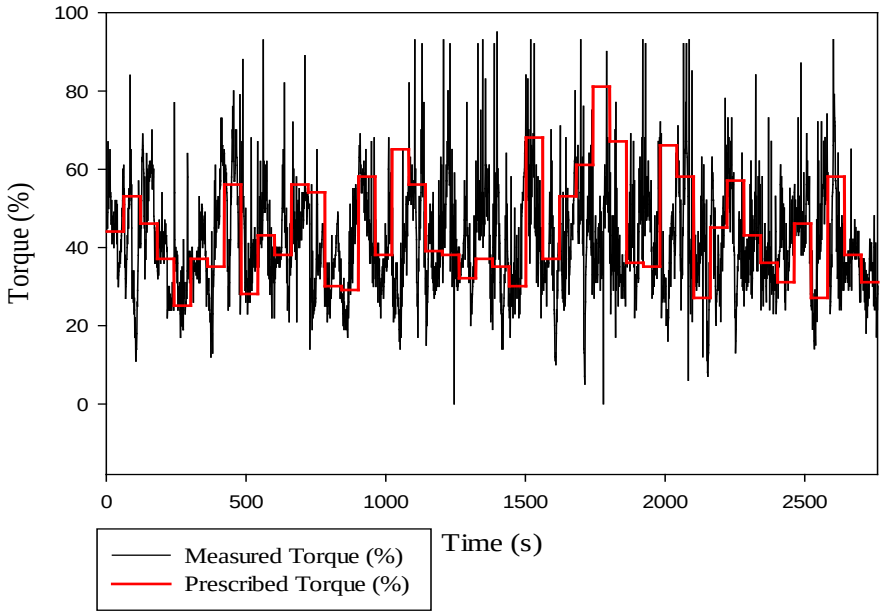

Figure 2.11 Recorded torque juxtaposed with down-sampled torque profile.

Table 2.2 Load profile characteristics comparison. Green boxes highlight the simplified parameter that is closest to the recorded parameter.

Category	**Recorded**	**Downsampled**	**Decimated**
Mean Load (%)	41.8	44.3	41.7
Minimum Load while operating (%)	5	25	29.3
Maximum Load (%)	95	81	53
First Quartile Load (%)	33	35	38
Median Load (%)	40	39	42
Third Quartile Load (%)	50	56	46
Mode Load (%)	37	37	29
Standard Deviation	13.1	13.3	5.8
Cross Correlation Coefficient with Recorded Signal	--	0.248	0.3202

The simplified load profile from downsampling has a similar mean, median and standard deviation and the same mode as the direct recording (Table 2.2). The minimum and maximum loads are less extreme in the simplified load profile as the downsampling

did not capture these outermost values. Although the statistical descriptors of the torque load profiles are similar, calculating the CCC between the two provides a value of only 0.25 at no time delay between patterns. This relatively low CCC reveals that performing the downsampling on the load profile has resulted in the loss of considerable information. This is entirely expected as the higher frequency components of the torque load profile have been removed and the number of discrete points has been reduced by a factor of 60 (from 1 sample/second to 1 sample/minute). On the other hand, it is encouraging that the CCC value is significantly above zero as a value close to zero would indicate that the new load profile was uncorrelated with the original. Thus, this downsampling has resulted in a profile significantly easier to recreate on a dynamometer that has similar statistical characteristics and has not become completely uncorrelated with the original torque load profile. On the other hand, the fact that even a load profile that varies every minute does not capture the noticed variability indicates that even higher speed dynamometer testing and higher frequency load analysis is necessary to truly describe agricultural loads.

Like the original loading pattern, the simplified loading has a tight cluster of values in the second quartile and more dispersed values in the remaining quartiles (Figure 2.12). Therefore, like the original torque loading, this simplified loading features a significant periods of time where the loads are near a base value. It also retains the dispersion of many samples where the loads are spread across a wide range of values above this base level up to values just over twice the base.

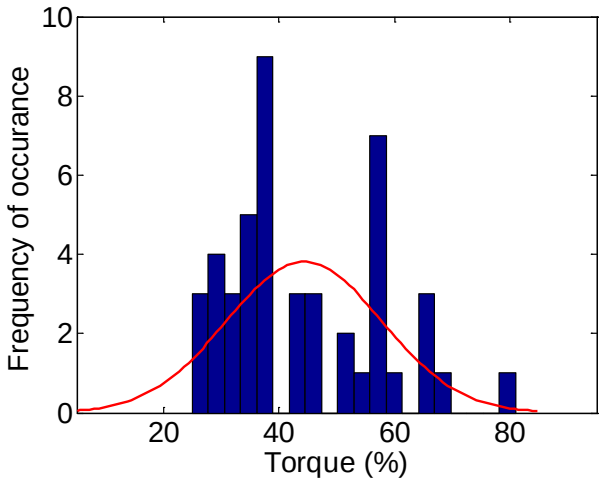

Figure 2.12 Histogram of simplified torque loading (blue) with the corresponding normal distribution (same mean and standard deviation) superimposed (red)

2.3.4 Load Re-creation

2.3.5 Replicating load profile on water brake dyno

Testing was performed on the on the dynamometer using the simplified torque load profile. The motors were set to run at full speed, and dynamometer resistance was varied to control torque to which the drivetrain was subjected. The torque load profile only expressed torque loads as a percent of the maximum torque load. By assigning a value for the maximum torque, the profile could be converted into a series of torque load values usable to control the dynamometer. The simplified torque load profile was recreated using the dynamometer in eight different tests. In four of these tests, the maximum torque was set to 136 N m, and in the other four, it was set to 102 N m.

The dynamometer was able to follow this simplified load profile with an average normalized root mean square error of 7.26% when normalized to the range of recorded data (Equation 2-1). As an example, figure 2 shows the desired load profile and the measured torque produced by the dynamometer in one of the loading tests.

$$NRMSE = \frac{\sqrt{\frac{\sum_{t=1}^{n}\left(\tau_{R,t} - \tau_{P,t}\right)^2}{n}}}{\tau_{R,max} - \tau_{R,min}} \times 100\% \qquad \text{Equation 2-1}$$

Where:

$\tau_{R,t} =$ recorded percent full torque at time t

$\tau_{P,t} =$ prescribed profile percent full torque at time t

$n =$ number of discrete time samples

$\tau_{R,max} =$ maximum recorded percent full torque

$\tau_{R,min} =$ smallest recorded percent full torque

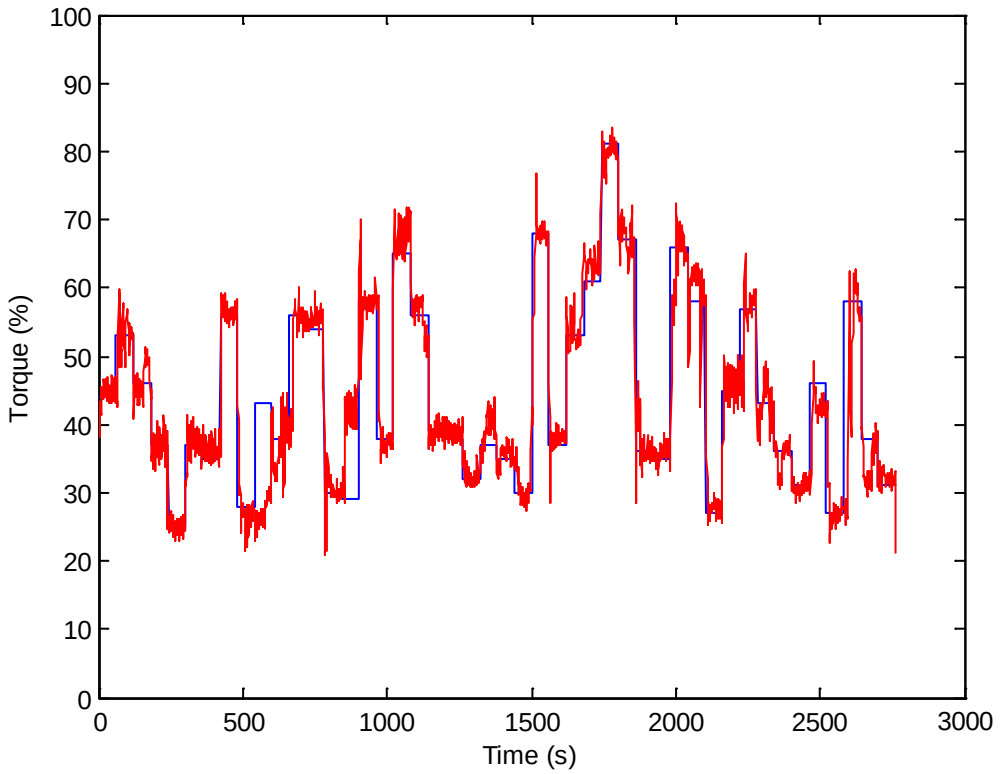

Figure 2.13 Example (Test number 3 – CCC = 0.91) of simplified torque load profile (blue) and dynamometer recording (red).

In order to quantify how similar the ideal simplified profile and those measured by the dynomometer during testing, the cross correlation coefficient was calculated. The lowest CCC value for any test was 0.843, while the highest was 0.96 and the average CCC for all tests was 0.914. With an average CCC over 0.9, it is apparent that the torque profiles recreated on the dynamometer closely matched the desired profile.

Table 2.3 shows the statistical characteristics and CCC values of the load profiles recreated using the dynamometer. The statistical characteristics indicate a close match between the desired and recreated load profiles. All of the tests maintained a tight cluster of torque loads in the second quartile and a wider dispersion of loads above the mean. Thus, the recreated torque load profiles were able to recreate one of the more notable features of the actual torque requirements recorded during the baling operation – a concentration of loads around a base torque level with increases in torque loading to over twice the base level.

Table 2.3 Comparison of the desired simplified load profile to that produced by the dynamometer in each of 8 tests.

Test No.	Simplified	1	2*	3	4*	5	6	7*	8*
CCC to Simplified	---	0.96	0.88	0.91	0.89	0.94	0.84	0.94	0.94
NRMSE (%)	6.15	8.24	9.13	9.54	5.96	9.23	5.96	5.96	6.15
Mean Torque Level (N m)	524†	54	41	54	41	54	54	41	41
Mean Load (%)	44	45	45	44	45	45	44	45	45
First Quartile Load (%)	35	35	36	34	35	35	34	35	35
Median Load (%)	39	41	40	40	40	41	39	41	41
Third Quartile Load (%)	56	55	56	56	55	55	55	56	56
Mode Load (%)	37	23	21	21	21	9	10	11	11

2.4 Conclusions

This study began by recording machine operational data collected at 1 Hz during a normal baling operation. This machine operational data was analyzed to determine characteristics of the torque requirements during this baling operation. A statistical analysis revealed that torque requirements seemed to cluster around a base value, but also half the torque values were widely dispersed above this base value and included values up to twice the base level. A time series analysis performed using a fourier transform revealed several periodic peaks in the required torque. One of the most prominent peaks appeared from the baler's plunger strikes. Other peaks at lower frequencies that were likely related to field conditions were less well defined. Both the statistical and time

* Marked tests are performed with maximum torque set as 102 N m. Other four tests are run with maximum torque set as 136 N m.

† This number is calculated using the max torque from the NTTL test data for the TG-305 and the mean torque loading percent calculated from the field recording.

series analysis of the recorded torque requirements confirmed that the loads imposed by an operation like baling are clearly not constant and actually quite complex in nature.

Use of the recorded torque profile for dynamometer testing required that the profile be simplified through downsampling. The downsampled signal retained the statistical features of the original recording, but it naturally eliminated information about high frequency torque variations like the baler plunger strike since the values were held constant for an entire minute. The simplified torque profile was then used in testing on the dynamometer. The dynamometer was successful in replicating the simplified torque profile as indicated by the high cross-correlation coefficients between the tests and the simplified profile and the similar statistical characteristics.

Naturally, future dynamometer testing could be improved by utilizing a dynamometer capable of recreating the 1 Hz torque profile as recorded by the tractor in field operation. However, given the limitations of the dynamometer used, the analysis techniques confirmed that the simplified torque loading profile used still maintained the statistical characteristics of the orignal profile. Improved dynamometer control could also improve the repeatability and reduce the NRMSE between the simplified signal and recorded signal.

A natural extension of this work is to utilize the analysis technique for many different operation types, field conditions and machinery sizes. With load recreation, another extension of this work would be to create a load profile model with parameters based on the analysis of many different operations. Both of these future work opportunities represent excellent methods to extend this work, but to be successful they must build on the foundation presented in this work for a single field operation.

CHAPTER 3: DRIVETRAIN PERFORMANCE

3.1 Introduction

Despite wide availability of hybrid passenger vehicles, hybrid drivetrains are uncommon in current agricultural equipment. Since agricultural loads are so much different from those seen by passenger vehicles, development of hybrid agricultural equipment requires that testing and modeling be performed to determine the feasibility of this type of drivetrain. Most diesel locomotives utilize an electric drivetrain that converts the full engine power to electricity to drive the electric wheel motors. The drivetrain developed for this testing is similar, but on much a smaller scale and with the added ability to store energy in a battery.

Tractors range in size from approximately 20 kW to over 300 kW, so when choosing a size of vehicle to test, considerations were made as to the size of tractor that would benefit from a hybrid drivetrain. The advantages of a hybrid drivetrain are in regenerative braking and handling changes in speed. Very large tractors are commonly used for heavy, constant draft loads. As such, very large tractors would not be able to reap the full benefit from a hybrid drivetrain. Small tractors are generally used for a variety of uses and therefore more likely to achieve efficiency gains from a hybrid drivetrain. Therefore, this testing utilized components for an approximately 20 kW tractor.

There were three areas of major concern for testing this drivetrain. The first is to determine how the hybrid drivetrain would be able to handle the variability associated with agricultural loads. Highly variable loads reduce efficiency in geared vehicles as the variations in loading affect the fuel-air mixture inside the engine creating conditions that lead to incomplete combustion. Since the hybrid drivetrain uses electric motors and has the capacity for energy storage, it is important to test how the tested drivetrain responds to this type of loading.

Furthermore, since the drivetrain uses the energy storage to handle variable loading, the second area of concern is what effect the capacity of the battery pack has on efficiency under the same load conditions.

The final area of concern is engine sizing. The power of a geared vehicle is limited directly by the power of the engine, meaning the engine must be able to handle all

loads to which it is subjected. Because the hybrid drivetrain has batteries for energy storage, the electric motors can produce more power than supplied by the generator for brief periods of time. Different load levels were tested to determine the effect of engine size on efficiency.

3.2 Materials and Methods

3.2.1 Equipment Utilized in the Experiment

3.2.1.1 Drivetrain

The drivetrain was a series hybrid system (Figure 3.1). Clark Material Handling Company donated an electric forklift (GEX 30) that was used for the wheel motors and motor controller. The forklift components were designed to operate with an 80 V battery pack. The motor controller was a ZAPI Dualac2 Power motor controller that converted the 80 V DC power into the correct 3 phase power for the motors and managed speed and directional control. The electrical power was converted to mechanical power by two Schabmüller 7.8 kW asynchronous motors. The output speed from each motor was reduced to the proper range for ground drive by a 29:1 gearbox, the S8C.3009.1 from PMP (Coseano, Italy). The output shafts of the gearboxes are normally bolted to the drive wheels. However, for this testing, the wheel motors were linked with the dynamometer via the speed increaser described in section 2.2.3.

Input energy to the system was supplied by diesel fuel which was converted to mechanical energy by a Perkins 404D-15 20 kW diesel engine. This engine was directly connected to a Polar Power 8340 generator (Polar Power, Carson, California).

This engine and generator were obtained as a single unit, the Polar Power 8340P-40515, which integrated the engine and related systems, the generator, charge controller, and the engine accessories necessary for operation, such as the cooling and exhaust packages. The engine/generator unit provided electrical power at 80 V to operate the drive motors and charge the battery pack during periods of low demand. The battery pack capacity was variable. Different configurations were used during testing, and details on the configurations are given in test procedures.

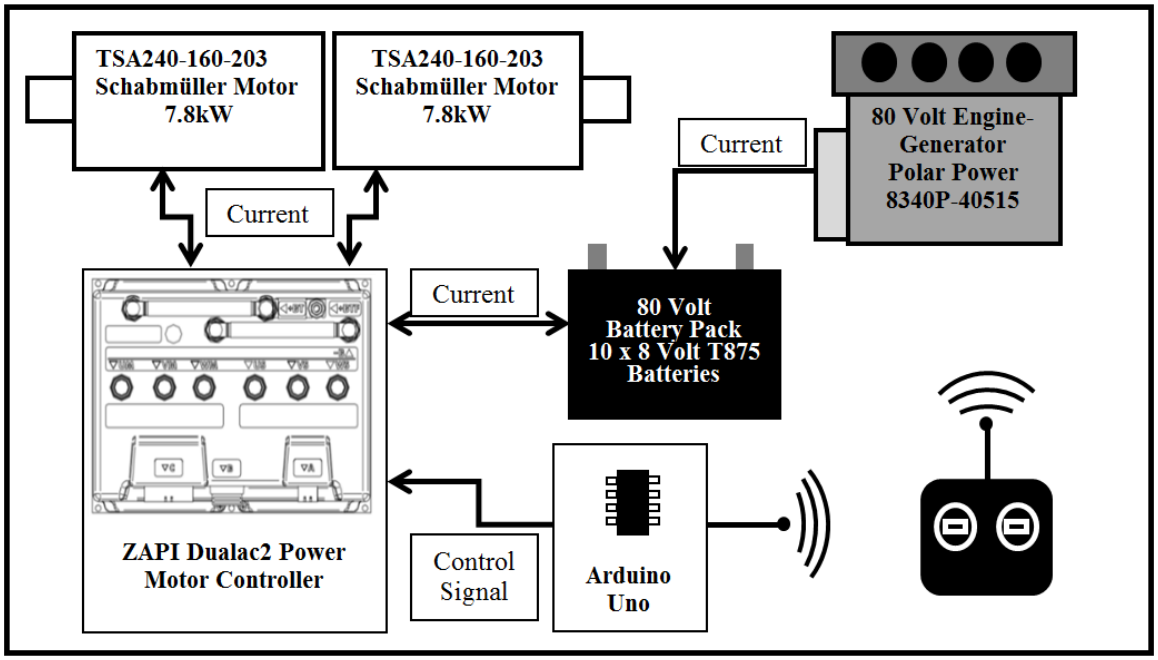

Figure 3.1 System diagram illustrating major components.

Figure 3.2 Hybrid drivetrain set up for testing. Polar power generator (left) and forklift frame connected to dynamometer (right).

3.2.1.2 Electrical Power Monitoring

The same DAQ board used in Chapter 2 to record torque also monitored the voltage at the battery pack, the current going from the generator to the batteries, and the current going from the batteries to the load. These signals were sampled at 100 Hz and averaged over one second to produce the value for that second.

The voltage of the battery pack was measured using a voltage divider to scale the voltage to within the range measurable by the DAQ. The currents were measured by LEM HASS 300-S (LEM USA, Milwaukee, WI) current transducers attached to the DAQ board. The current and voltage were both recorded in LabView.

3.2.1.3 Fuel Consumption Monitoring

The fuel consumption was monitored by drawing fuel from an 18.9 liter fuel tank placed on a digital scale adjacent to the engine, and measuring the combined weight of the fuel and tank. The Ohaus CD-11 scale (Ohaus, Florham Park, New Jersey) reported fuel weights to the nearest 25 grams every second. This data was logged from the scale by serial connection and synchronized with the electrical power data using system time on the computer.

3.2.1.4 Radio control

Radio control was implemented in order to control the electric motor output remotely. A FlySky FS-T6B transmitter (FlySky, DongGuan, China) was used to send an RC signal to the paired FS-R6B radio receiver. An Arduino Uno microcontroller powered the radio receiver, and measured the RC pulse signal from a single channel of the receiver. The pulse length was measured and mapped to an analog voltage control signal for the Zapi motor controller with 5 V for stationary, and 0.25 V for full speed. The Arduino also used relays to control the motor rotation direction, and accelerator enable safety switches on the motor controller. During the efficiency tests presented here, the radio control was used to continuously request the maximum speed (1850 RPM) from the motors. Utilizing radio control for the motor speed provided a simple way to start and stop tests, and enabled the test operator to control the system from the safety of the instrumentation station.

3.2.2 Test design

The experiment was a 2x2x2 factorial design. Every combination of two different load levels, two different battery pack sizes, and two different loading patterns were tested for a total of eight different conditions. The test began with the battery pack fully charged and the generator in "Auto" mode to allow it to shut off when the battery pack was charged. After the loading period, the generator was allowed to run until the batteries were charged and automatic shutdown occurred. This was done to ensure that the batteries were at the same state of charge at the start and end of the test.

3.2.2.1 Battery pack

The battery pack was tested at two capacities, 170 Amp-hours and 340 Amp-hours. The 170 Amp-hour battery pack was created using 10 T875 8 volt, 170 Amp-hour Trojan deep cycle lead-acid batteries connected in series. This produced an 80 volt (nominal) battery pack with a capacity of 170 Amp-hours. The second battery pack was two of these 80 volt packs connected in parallel for a total of 20 T875 batteries, and 340 Amp-hours.

3.2.2.2 Load levels

The two load levels were chosen such that the test run would have an average load value of 54 N m of torque (HIGH load) and 41 N m of torque (LOW load). The HIGH load tests were scaled using the maximum continuous torque of the two Schabmüller Motors which was 136[‡] N m. The LOW load tests were scaled down such that the maximum torque value was 75% of the HIGH load test for a maximum torque of 102 N m. The ZAPI speed controller was set to run at full speed, and the load resistance was varied until the desired torque value was attained. At the requested motor test speed of 1850 rpm, this corresponded to 10.4 kW for the HIGH load and 7.8 kW for the LOW load.

[‡] There are several gear increases before this torque is as measured at the dynamometer. This is the maximum continuous torque after being scaled through these increases.

3.2.2.3 Load patterns

Two load patterns were also tested to determine how the drivetrain responded to variable 'real life' loading versus idealized constant average loading (Figure 3.3). The constant average loading was used to calculate the power values referenced in the section above. The variable load pattern had periods of high and low demand following the load pattern developed in Chapter 2.

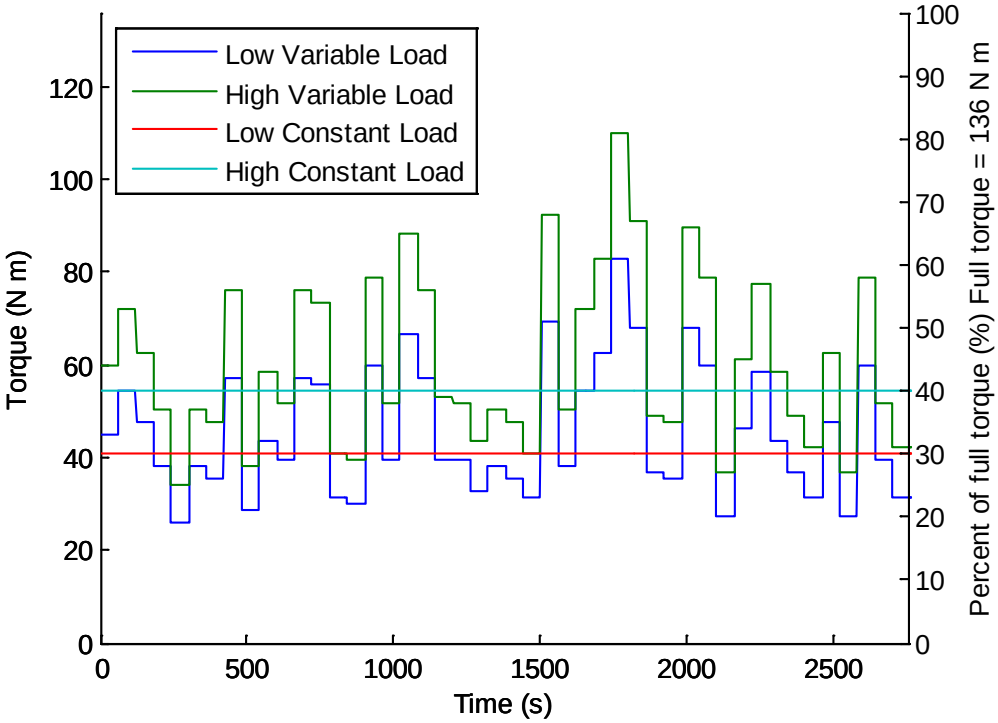

Figure 3.3 Graph of the load patterns and levels tested, where full torque is the maximum continuous torque of the motors, 136 N m.

3.2.2.4 Tested Scenarios

The 2x2x2 factorial design resulted in 8 different testing scenarios; (Table 3.1) two replications were performed of each test scenario in a randomized order. In addition to the factor levels for each scenario, the table also includes an abbreviation for each scenario that will be used in results presentation and discussion. At least two tests were performed for each test scenario except for scenario number 8. A data recording error occurred in one of the tests of this scenario so only one test was available for processing.

The error was not discovered until post-processing the data after the drivetrain had been dismantled and was no longer available for testing.

Table 3.1 Drivetrain configurations tested.

Scenario Number	**1**	**2**	**3**	**4**	**5**	**6**	**7**	**8**
Chart Abbreviation	Small Low Fixed	Small Low Variable	Large Low Fixed	Large Low Variable	Small High Fixed	Small High Variable	Large High Fixed	Large High Variable
Battery Size (A hr)	170	170	340	340	170	170	340	340
Load Level (N m)	41	41	41	41	54	54	54	54
Load Pattern	Fixed	Variable	Fixed	Variable	Fixed	Variable	Fixed	Variable
Number of Tests	2	2	2	2	2	3[§]	2	1

3.3 Results and Discussion

To determine what variables significantly affected the drivetrain efficiency, the data were subjected to statistical analysis. An analysis of variance (ANOVA) was calculated for several dependent variables – the efficiency of portions of the drivetrain – with the independent variables corresponding to the factors: load level, battery size, and load pattern. The ANOVA results were analyzed to determine if there were interaction effects. The null hypothesis was that there was no interaction between any factors, with the alternative hypothesis that there was some interaction between factors. The level of significance was set at $\alpha = 0.05$. For all the tests in this chapter, the calculated p-value is greater than the level of significance so the null hypothesis was not rejected and it was concluded that there is no interaction between factors.

After concluding there was no interaction, the main effects of the individual factors were analyzed. For each factor, the null hypothesis was that the effects due to different levels of that factor were equal; the alternative hypothesis was that the effects were not equal – that there was a significant difference in the results due to the level of that factor. The level of significance was set at $\alpha = 0.05$. These results are discussed in depth in the subsection dedicated to each portion of the drivetrain.

[§] One extra test was performed for this testing scenario; the data was retained and added to the analysis.

3.3.1 Overall Efficiency

The overall efficiency is the ratio of the energy recorded at the dynamometer divided by the energy in the fuel consumed. The energy recorded at the dynamometer was calculated by finding the power consumption from the measured torque and rotational speed at the dynamometer, then taking the trapezoidal integration of the power. The power was recorded as a series of discrete measurements at regularly timed intervals throughout the test. Since the energy is calculated as the area under the curve bounded by the power data, the points must be connected into a continuous curve. The curve was formed by linearly interpolating between measurements and finding the area of the resulting trapezoid. The fuel energy was calculated from the energy density of the diesel fuel, and the weight of the fuel consumed. The density and volumetric energy content values used in these calculations were taken from Brown and Brown (2003). Figure 3.4 summarizes the mean drivetrain efficiencies for each of the 8 tested conditions.

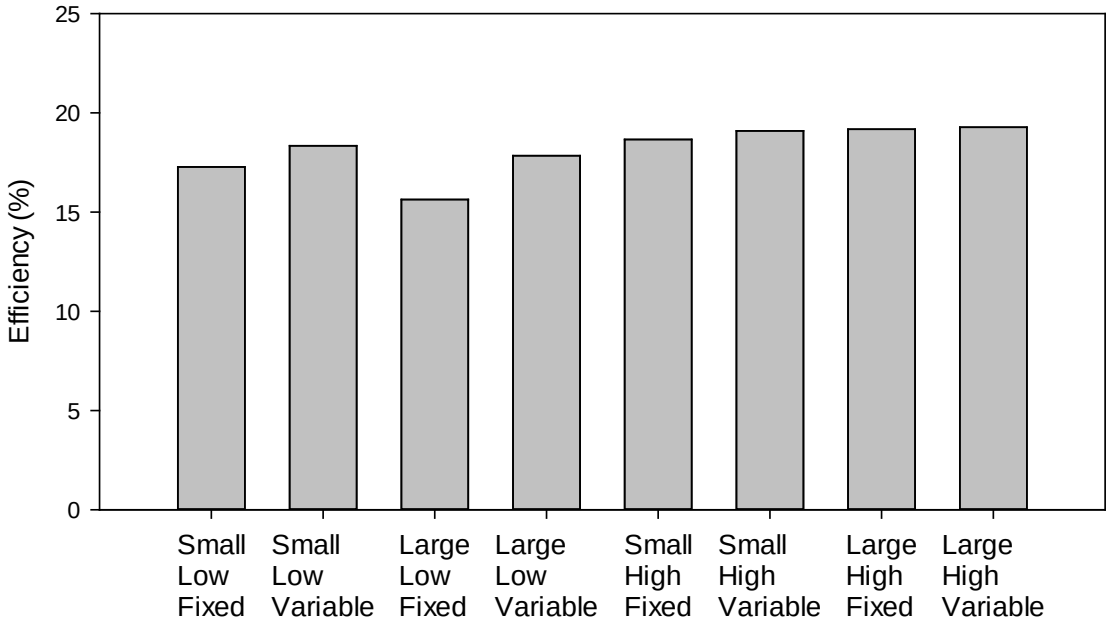

Figure 3.4 Overall efficiencies averaged within each test category.

A 2x2x2 ANOVA was calculated on the overall efficiency of the drivetrain. The main effects and interactions between overall efficiency and load level, variability and battery

size were calculated. When considering the ANOVA results, the P-value for all interaction effects is greater than 0.2 indicating that interaction between variables has little effect on the result. Looking at the main factors, the P-value due to battery pack size is also very high at 0.49 which indicates that changing battery pack size also had limited effect.

Table 3.2 ANOVA table for overall efficiency.

Source	DF	Type 1 SS	Mean Square	F Value	Pr > F
Load Level	1	12.34643906	12.34643906	9.91	0.0136
Battery Size	1	0.65436339	0.65436339	0.53	0.4893
Load Level*Battery Size	1	1.78178478	1.78178478	1.43	0.266
Load Pattern	1	3.84177353	3.84177353	3.08	0.1172
Load Level*Load Pattern	1	1.69810307	1.69810307	1.36	0.2766
Battery Size*Load Pattern	1	0.19523913	0.19523913	0.16	0.7026
Load Level*Battery Size* Load Pattern	1	0.50014031	0.50014031	0.4	0.544

Because battery pack size had very little effect, considering it in the ANOVA adds an unnecessary variable that does not fit the model. This adds complexity to the analysis and can add noise to the effects of other variables. After noticing this feature in the data, the Applied Statistics Laboratory at the University of Kentucky removed the battery size factor from the analysis. Therefore, the ANOVA was recalculated with batteries removed, and the results are summarized in Table 3.3. The low p value for the effect of load level indicates that there is not enough evidence to say that the efficiency of the drivetrain is unaffected by load level.

Table 3.3 ANOVA table for overall efficiencies with battery pack size removed from the analysis.

Source	DF	Type 1 SS	Mean Square	F Value	Pr > F
Load Level	1	12.34643906	12.34643906	11.24	0.0058
Load Pattern	1	3.44009756	3.44009756	3.13	0.1022
Load Level*Load Pattern	1	2.01427056	2.01427056	1.83	0.2007

The plot of the overall efficiency by load level (Figure 3.5) shows that, on average, the drivetrain was more efficient at the HIGH load level.

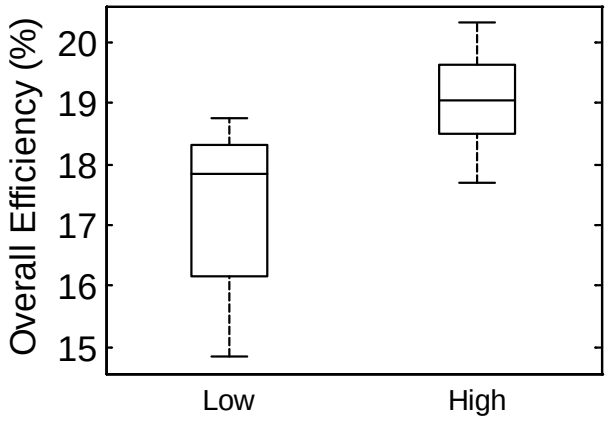

Figure 3.5 Comparing overall efficiency separated by load level.

3.3.2 Engine and Generator Efficiency

Because the power and energy were monitored at several points throughout the drivetrain, it is possible to break down the overall efficiency by the component in which the losses occur. The efficiency of the fuel consumption of the generator to the electrical output of the generator is shown in Figure 3.6. The efficiency of the engine and generator does not change significantly for any of the categories of tested parameters. An ANOVA was calculated, and there was not enough evidence to say the average efficiencies are significantly different between the tested factors at the level of significance $\alpha = 0.05$ (Table 3.4).

Table 3.4 ANOVA table for engine and generator efficiency

Source	DF	Type I SS	Mean Square	F Value	Pr > F
Load_Level	1	4.5914	4.5914	3.26	0.0962
Variable	1	0.3111	0.3111	0.22	0.6469
Load_Level*Variable	1	1.2673	1.2673	0.9	0.3617

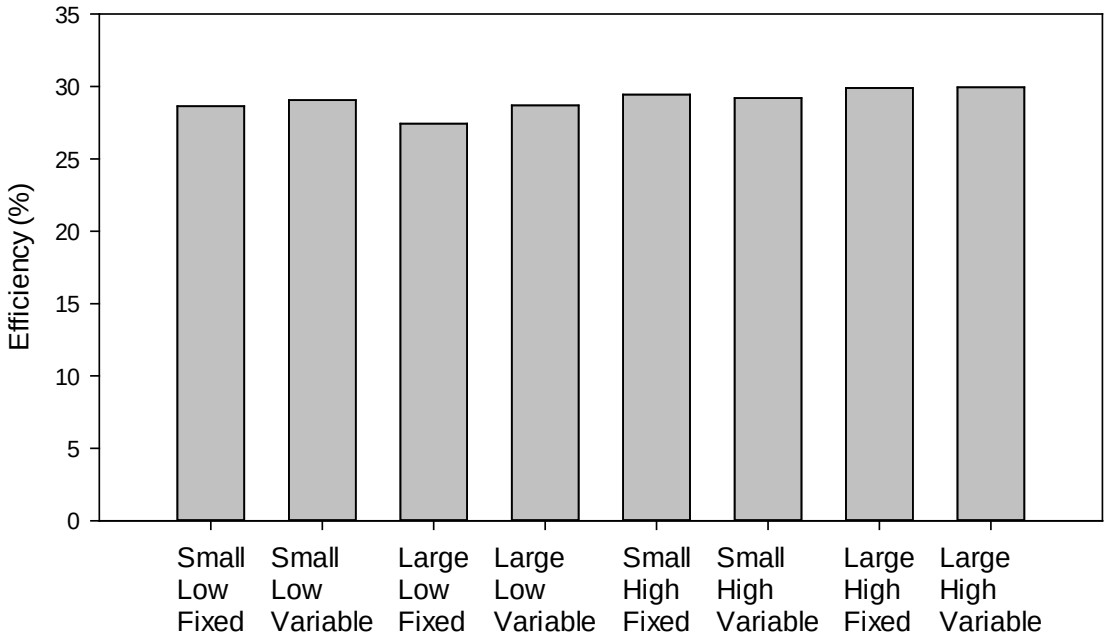

Figure 3.6 Generator efficiencies averaged within each test category.

3.3.3 Motor Efficiency

The efficiency of the electric motors as determined by electrical energy leaving the batteries to the mechanical energy measured at the dynamometer is shown in Figure 3.7. This efficiency was a cumulative measure that included the motor controller/inverters as well as the motors. The motor efficiency measurement varied more than the efficiency of the generator. The efficiency of the motors, however, does not change significantly for any of the categories of tested parameters. An ANOVA was calculated, and there was not enough evidence to say the average efficiencies are significantly different.

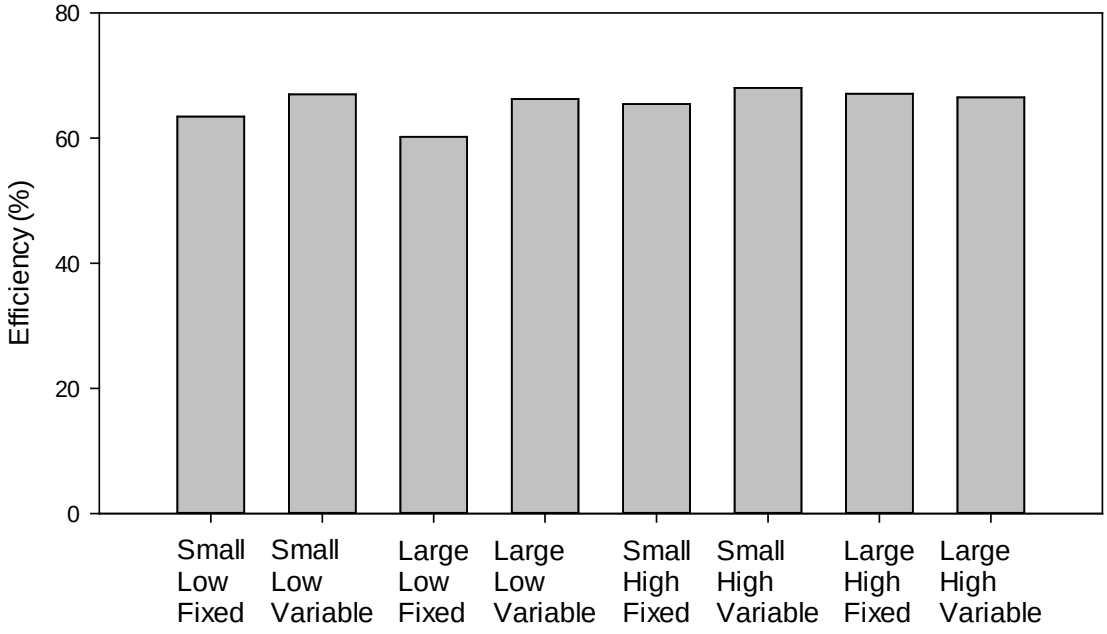

Figure 3.7 Motor efficiencies averaged within each test category.

3.3.4 Battery Efficiency

The battery efficiency in this context is the ratio of the amount of energy leaving the batteries to the amount of energy entering the batteries. Figure 3.8 summarizes the mean battery efficiencies for each of the 8 tested conditions.

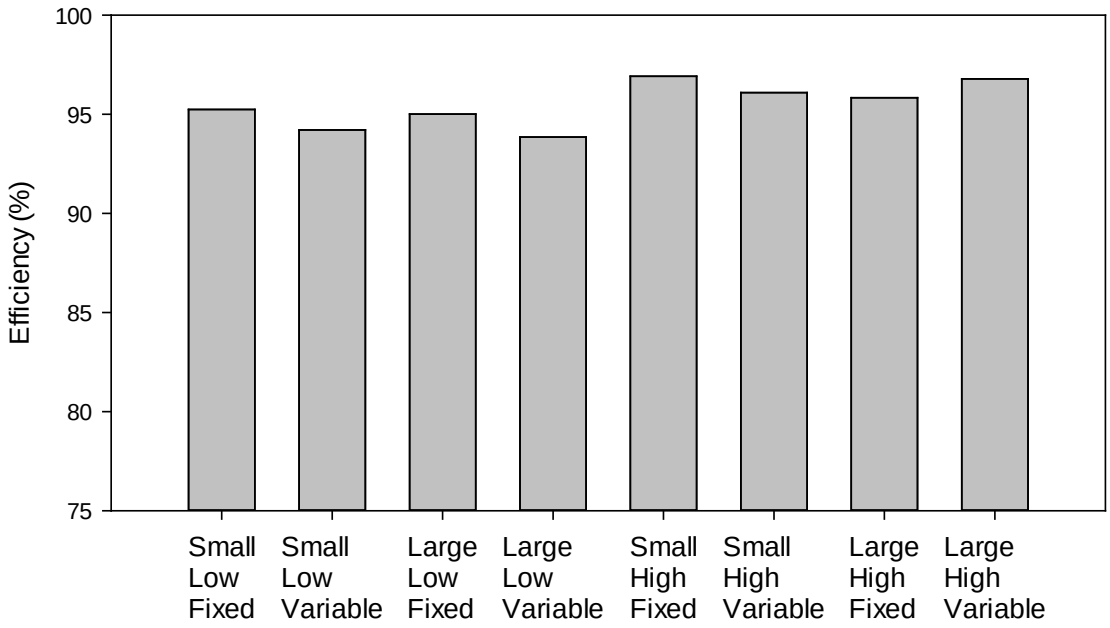

Figure 3.8 Battery efficiencies averaged within each test category.

As with the generator and motor efficiencies, an ANOVA was calculated to determine the treatment effects on the efficiency of the batteries (Table 3.5). The P-value due to battery size is high. As with the overall efficiency, the Applied Statistics Laboratory recommended removing this factor. Therefore, the ANOVA was recalculated with batteries removed from the analysis (Table 3.6).

Table 3.5 ANOVA table for battery efficiencies

Source	DF	Type I SS	Mean Square	F Value	Pr > F
Load Level	1	12.17137656	12.17137656	3.67	0.0917
Battery Size	1	0.31603068	0.31603068	0.1	0.7655
Load Level* Battery Size	1	0.00049283	0.00049283	0	0.9906
Load Pattern	1	1.68625656	1.68625656	0.51	0.4961
Load Level* Load Pattern	1	0.79159435	0.79159435	0.24	0.6383
Battery Size* Load Pattern	1	0.52371521	0.52371521	0.16	0.7015
Load Level* Battery Size* Load Pattern	1	0.84466308	0.84466308	0.25	0.6274

When batteries are removed from the analysis, the p-value for load level is below the level of significance $\alpha = 0.05$. This indicates that load level is a significant factor in efficiency of the batteries.

Table 3.6 ANOVA table for battery efficiencies with battery pack size removed from the analysis.

Source	DF	Type 1 SS	Mean Square	F Value	Pr > F
Load Level	1	12.17138	12.17138	5.17	0.0422
Load Pattern	1	1.459868	1.459868	0.62	0.4464
Load Level* Load Pattern	1	0.973676	0.973676	0.41	0.5324

The average battery efficiency is actually higher for the HIGH load level than for the LOW load level (Figure 3.9).

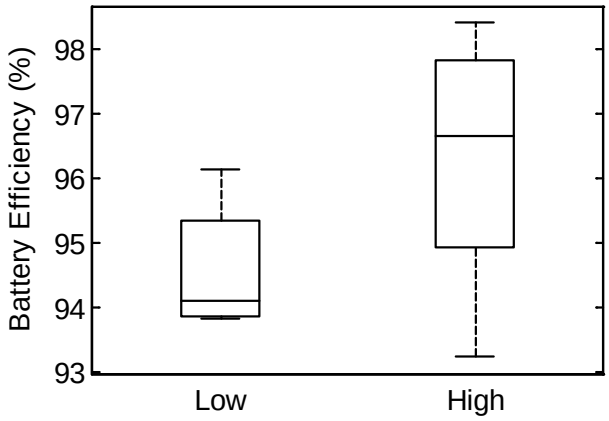

Figure 3.9 Battery efficiency separated by load level.

3.3.5 Generator Operating Time

In addition to the other variables measured, the percent of the test time that the generator was running was recorded. The generator could run for a short time after finishing the dynamometer test to finish fully charging the batteries. This time was also counted when considering operating time or utilization percentage of the generator. Because the drivetrain can run on battery power during periods of low demand, the engine can shut off automatically if the batteries are charged. The utilization of the generator is somewhat indicative of fuel consumption over the course of the test, but in a different way than the fuel consumption. The energy to run the tests had to be generated before the end of the test; although lower utilization values ran the engine for a shorter amount of time, it was under a heavier load. An ANOVA was calculated for the operating time as measured. Battery pack size, once again, had a very high P-value, so it was not considered in the results presented in Table 3.7. The P-values for load level and load pattern are both below the $\alpha = 0.05$ level of significance so both variables are significant factors that affect operating time of the generator.

Table 3.7 ANOVA table for utilization with battery pack size removed from the analysis.

Source	DF	Type 1 SS	Mean Square	F Value	Pr > F
Load Level	1	0.03184	0.03184	21.8	0.0005
Load Pattern	1	0.013246	0.013246	9.07	0.0108
Load Level* Load Pattern	1	0.000701	0.000701	0.48	0.5017

As illustrated below, the generator runs a higher percentage of the time during the high load level tests. The high load level consumes more energy than the lower level test and the generator would need to run for a higher percentage of the test period on average in order to produce the extra energy.

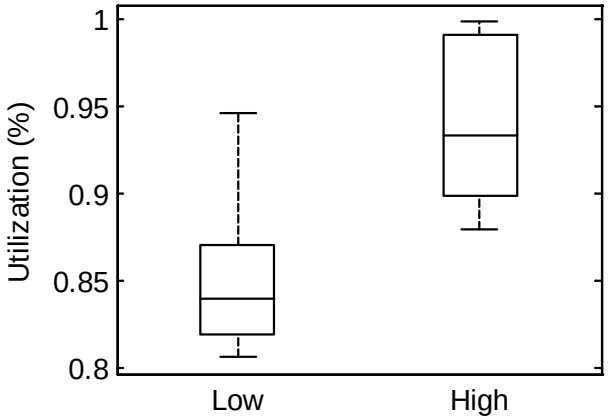

Figure 3.10 Box plot of generator operating time versus load level.

The generator runs a lower percentage of the time during variable load tests as seen in the figure below. The variable test was able to take advantage of the energy storage abilities of the hybrid drivetrain. Even though the amount of time the generator was running was significantly different between constant and variable tests, earlier results imply that the generator efficiency was not significantly different. This would indicate that during the variable test, the generator was under heavier loads for a shorter period of time.

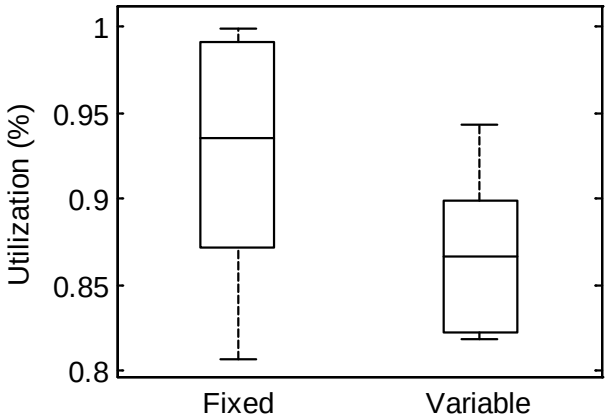

Figure 3.11 Box plot of generator operating time versus load pattern.

Further analysis of the generator operating time reveals that there appears to be some correlation between utilization, and overall efficiency (Table 3.8). However, correlation does not appear to be very strong, and the linear model is not a good fit for the data based on the R^2 value (Figure 3.12).

Table 3.8 Linear regression model between uptime and efficiency.

Source	
DF	1
Type 1 SS	8.00237673
Mean Square	8.00237673
F Value	4.87
Pr > F	0.0444
R-Square	0.258269
Coeff Var	7.057383
Root MSE	1.281246

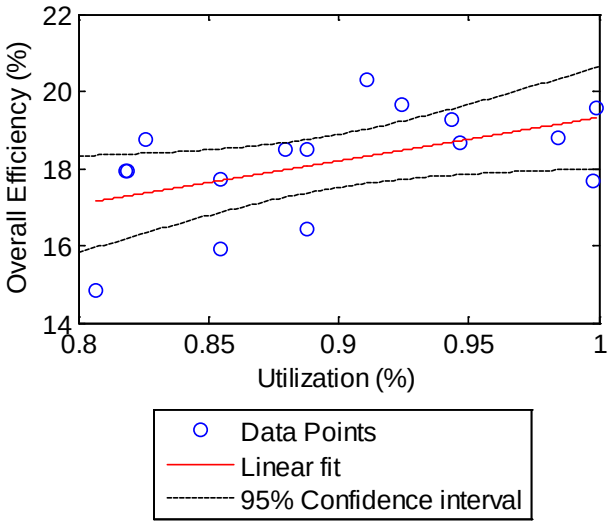

Figure 3.12 Trend line comparing percent of test engine running with overall efficiency.

3.3.6 Average Voltage

The arithmetic mean voltage was also calculated for the length of the test. During testing, the voltage of the battery pack dropped whenever the generator could not meet the energy demand or while the generator shut off. Conversely, the voltage peaked during low demand or when being actively charged after loading ceased.

A general linear regression was performed between the average voltage and the various efficiencies. There did not appear to be a significant correlation between the average voltage of the system and the efficiency of the system.

The average voltage was significantly affected by load pattern of the test as represented by the P-value less than $\alpha = 0.05$ level of significance (Table 3.9). When the drivetrain was subjected to variable loading, the average voltage was lower (Figure 3.13). This is likely related to the larger percentage of time spent with the generator off (lower utilization) as was seen in Figure 3.11.

Table 3.9 ANOVA table for average voltage with battery pack size removed from the analysis.

Source	DF	Type 1 SS	Mean Square	F Value	Pr > F
Load Level	1	2.686944	2.686944	0.81	0.3851
Load Pattern	1	29.96717	29.96717	9.06	0.0109
Load Level* Load Pattern	1	11.01505	11.01505	3.33	0.093

The average voltage for the fixed load tests was just below the absorption (active charging) voltage of 94 to 98 V for the 80 V battery pack. Combined with the high utilization associated with the fixed load tests, it appears the hybrid system was at a high state of charge during the fixed load test, but not high enough for the generator to shut off. The power consumed by the load balanced the power generated.

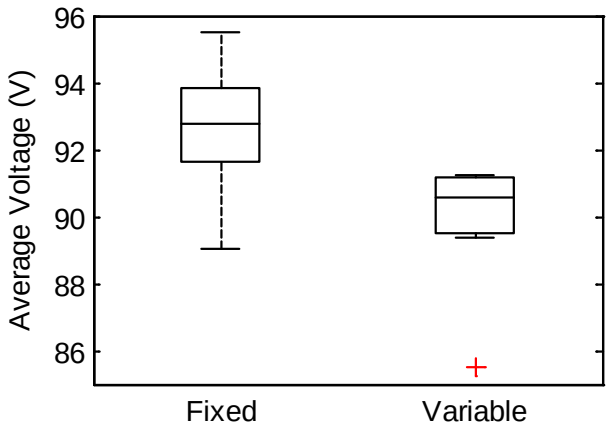

Figure 3.13 Boxplot of average voltage versus test type.

3.3.7 Discussion

The Perkins Engine Specification Manual states that the 404D-15 engine at 2800RPM generates 24.6 kW of power while consuming 73.6 kW worth of fuel for an efficiency of 33.4%. The average efficiency of the fuel to electrical energy conversion for this drivetrain was 29%. This indicates that the generator portion of the engine/generator combination had an efficiency of 86.8%. The efficiency of the drivetrain independent of the engine was therefore approximately 54.3%.

The calculated efficiency values throughout this chapter assume that there was no energy loss between the wheel motors and the dynamometer. In reality there were losses, due to the speed increaser. These losses do not affect the relative conclusions, as the losses were applied to all test scenarios. Since the speed increaser had two stages of roller chains, each approximately 98% to 99% efficient and gearbox estimated at 96% to 98% efficient, the cumulative efficiency of the speed increaser would be no lower than 92%. Despite the inefficiencies associated with the dynamometer, the drivetrain produced 1.83 kW h l^{-1} at 40% of full torque load as measured at the dynamometer. For comparison, a similarly sized tractor[**] was found by the NTTL to produce 1.92 kW h l^{-1} at 44% of full load. This is within the margin of error caused by the speed increaser.

One limitation of the drivetrain to be addressed in further iterations is the charge control of the batteries. The generator had an integrated charge controller that determined how much current was allowed to go to the load, and monitor the state of charge of the batteries. Since the generator was not optimized for use with a hybrid drivetrain, it was not able to properly decouple the engine from the load as originally intended. The generator tried to keep the batteries charged to 100% at all times. This resulted in the generator actually following the load during a variable load test as though the batteries were negligible capacity with the exception of shutting down when it determined the batteries were full (Figure 3.14). More advanced power management strategies are needed to take full advantage of the battery storage.

[**] The Case IH DX 48 Diesel had a maximum power of 30.56 kW. The full test report is available at: http://tractortestlab.unl.edu/c/document_library/get_file?uuid=3e91826e-a983-4714-8c87-a2030517e840&groupId=4805395&.pdf

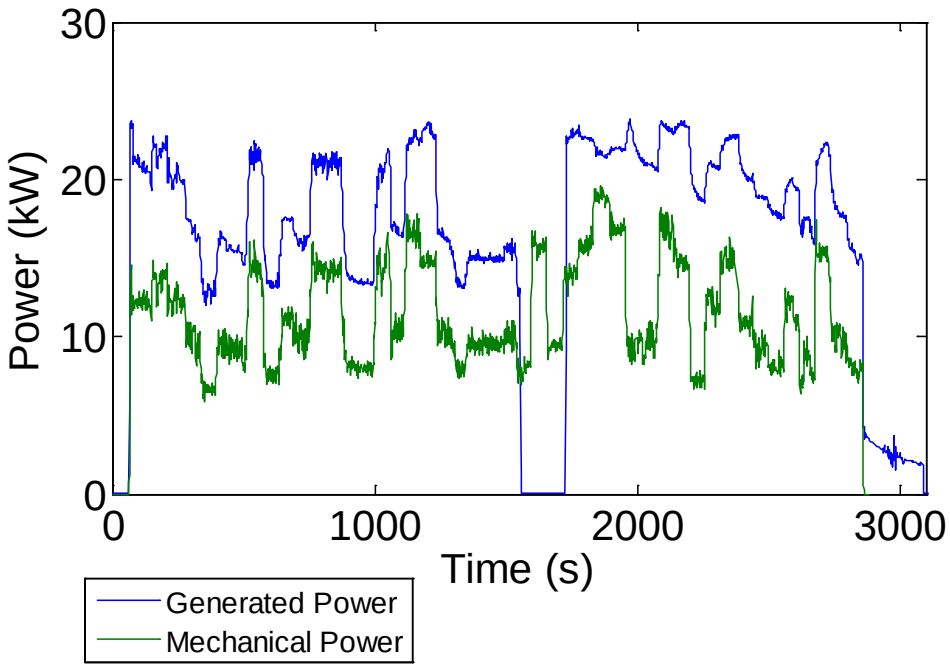

Figure 3.14 Power generated and power recorded at the dynamometer for an example variable load test.

3.4 Conclusions

3.4.1 Battery

Battery size was not a contributing factor to the efficiency of any part of the drivetrain as tested. There does not appear to be an advantage to the larger battery pack size for the tested conditions. A smaller battery pack could be used to limit weight and expense. A lower energy battery pack could be used to further reduce weight and price, but with a smaller battery, the length of time that the tractor would be able to operate with the engine off would be limited. Further testing would be necessary to determine the optimal battery size to provide energy for load leveling.

3.4.2 Efficiency

The efficiency of the drivetrain was unaffected by whether the test was variable or constant. The ability of the batteries to be used for load leveling is an advantage that this drivetrain has over a mechanical drivetrain. It allows the efficiency to stay the same between variable and constant load patterns.

Regardless of load pattern or load level, the generator efficiency was extremely consistent. The generator has to generate the energy used throughout the duration of the test at some point regardless of load conditions. The energy losses due to variations in load level, and the times in which the generator was shut off were handled by the battery. Electric motors are generally more efficient when operated close to rated power, but over the course of this test, the efficiency of the motors did not change significantly either. The efficiencies associated with the generator and the motors are relatively stable. As such, the variability in the efficiency due to different load conditions is reflected in the charging and discharge efficiency of the batteries. The factors that most affected the efficiency of the batteries were the speed and extent to which the batteries are drained and recharged.

3.4.3 Utilization

Utilization is a result of the loading pattern. Observation of the test recordings shows that the generator was most likely to shut off and had a lower utilization value during variable loading tests. When there was a period of low demand in the variable load profile, the generator shut off. Similarly, the generator would shut off for longer periods of time during the constant LOW load value test as well. The results of the ANOVA test support these observations. The longer amount of time that the generator was shut off resulted in draining more energy from the batteries. Draining more energy means that energy has to be replaced and recharged. It would follow that the tests with higher utilization percentage would generally have a higher efficiency than tests with lower utilization. The linear trend between utilization and overall efficiency and the fact that the correlation of these factors is significant at $\alpha=0.05$ supports this conclusion.

3.4.4 Overall

While the serial hybrid drivetrain has the most advantage in operations that involve frequent change of direction, the dynamometer used did not have the ability to supply negative torque to simulate regenerative braking, nor did the variable load pattern include any negative torque loads. Despite these limitations, the efficiency of the drivetrain was not significantly affected by whether the load pattern was variable or constant, which indicates that the hybrid drivetrain effectively took advantage of its energy storage ability.

The prototype drivetrain efficiency was comparable with the efficiency of a similar sized tractor under equivalent loading. Although the geared transmission was slightly more efficient, there is still significant room for optimization of the power management within the drivetrain.

The drivetrain was not only able to handle the variable loads of agricultural operations, but handled the highly variable agricultural load as efficiently as a constant load requiring the same average power.

REFERENCES

Alcock, R. (1983). Battery Powered Vehicles for Field Work. *Transactions of the ASAE*, 4.

American Society of Agricultural and Biological Engineers. (2011). ASAE D497.7 Mar2011 Agricultral Machinery Management Data *ASABE Standards 2011*: American Society of Biological and Agricultural Engineers.

Blackmore, S., Have, H., & Fountas, S. (2002). A specification of behavioural requirements for an autonomous tractor. *Automation technology for off-road equipment, edited by Zhang, Q. ASAE Publication*, 33-42.

Brown, R. C., & Brown, T. R. (2003). The Biorenewable resource base. *Biorenewable Resources: Engineering New Products from Agriculture, Second Edition*, 69.

Buning, E. A. (2010). *Electric drives in agricultural machinery-approach from the tractor side.* Paper presented at the Club of Bologna, 21 Annual Meeting, http://www. clubofbologna. org/ew/documents/knr_buning. pdf, last accessed January.

Coffman, B. A., Kocher, M. F., Adamchuk, V. I., Hoy, R. M., & Blankenship, E. E. (2010). Testing Fuel Efficiency of a Tractor with a Continuously Variable Transmission. *26*(1).

Emmi, L., Paredes-Madrid, L., Ribeiro, A., Pajares, G., & Gonzalez-de-Santos, P. (2013). Fleets of robots for precision agriculture: a simulation environment. *Industrial Robot: An International Journal, 40*(1), 41-58.

Goering, C. E., & Cho, H. (1988). Engine model for mapping BSFC contours. *Mathematical and Computer Modelling, 11*(0), 514-518. doi: http://dx.doi.org/10.1016/0895-7177(88)90546-8

Hansen, A., Walker, A., Lyne, P., & Meiring, P. (1986). Power demand mapping of tractor operations. *Transactions of the ASAE, 29*(3), 656-660.

Hansson, P. A., Lindgren, M., Nordin, M., & Pettersson, O. (2003). A METHODOLOGY FOR MEASURING THE EFFECTS OF TRANSIENT LOADS ON THE FUEL EFFICIENCY OF AGRICULTURAL TRACTORS. *19*(3), 251.

Harris, H. D. (1992). Prediction of the torque and optimum operating point of diesel engines using engine speed and fuel consumption. *Journal of Agricultural Engineering Research, 53*(0), 93-101. doi: http://dx.doi.org/10.1016/0021-8634(92)80076-5

Harris, H. D., & Pearce, F. (1990). A universal mathematical model of diesel engine performance. *Journal of Agricultural Engineering Research, 47*(0), 165-176. doi: http://dx.doi.org/10.1016/0021-8634(90)80038-V

Hori, Y. (2004). Future Vehicle Driven by Electricity and Control -- Research on Four-Wheel-Motored "UOT Electric March II". *IEEE TRANSACTIONS ON INDUSTRIAL ELECTRONICS, 51*(5).

Howard, C. N., Kocher, M. F., Hoy, R. M., & Blankenship, E. (2013). Testing the Fuel Efficiency of Tractors with Continuously Variable and Standard Geared Transmissions.

Hoy, R. M., Rohrer, R., Liska, A., Luck, J. D., Isom, L., & Keshwani, D. R. (2014). Agricultural Industry Advanced Vehicle Technology: Benchmark Study for Reduction in Petroleum Use.

Karner, J., Prankl, H., & Kogler, F. (2012). *Electric drives in agricultural machinery.* Paper presented at the Energy, biomass and biological residues. International Conference of Agricultural Engineering-CIGR-AgEng 2012: Agriculture and Engineering for a Healthier Life, Valencia, Spain, 8-12 July 2012.

Kenneth, J. S., Joachim, S., Bin, S., & Edwin, R. K. (2013). *Tractor Power for Implement Operation--Mechanical, Hydraulic, and Electrical: An Overview*. Paper presented at the 2013 Agricultural Equipment Technology Conference, Kansas City, Missouri, USA. http://elibrary.asabe.org/abstract.asp?adid=42518&t=6

Lodge, C., & Burgess, S. (2002). A model of the tension and transmission efficiency of a bush roller chain. *Proceedings of the Institution of Mechanical Engineers, Part C: Journal of Mechanical Engineering Science, 216*(4), 385-394.

Mousazadeh, H., Keyhani, A., Javadi, A., Mobli, H., Abrinia, K., & Sharifi, A. (2010). Optimal Power and Energy Modeling and Range Evaluation of a Solar Assist Plug-in Hybrid Electric Tractor (SAPHT). *53*(4).

Myong-Jin, R., Sin-Woo, K., Sun-Ok, C., Yong-Joo, K., Dae-Hyun, L., & Chang-Hyun, C. (2013). *Load Characteristics of 30 and 75 kW Agricultural Tractors during Field Operations*. Paper presented at the 2013 Kansas City, Missouri, July 21 - July 24, 2013. http://elibrary.asabe.org/abstract.asp?adid=43763&t=5

Myong-Jin, R., Sun-Ok, C., Yong-Joo, K., Dae-Hyun, L., Chang-Hyun, C., & Kyeong-Hwan, L. (2012). *FFT Analysis of Load Data during Field Operations Using a 75-kW Agricultural Tractor*. Paper presented at the 2012 Dallas, Texas, July 29 - August 1, 2012. http://elibrary.asabe.org/abstract.asp?adid=42048&t=5

N.L. Buck, H. A. H., M. Resen, R. Alcock. (1983). Electric Vehicle Designs for Agricultural Applications. *Transactions of the ASAE*.

Pitla, S., Luck, J., & Shearer, S. (2010). *Multi-Robot System Control Architecture (MRSCA) for Agricultural Production.* Paper presented at the American Society of Agricultural and Biological Engineers International Meeting, Pittsburgh, PA, June.

Pollet, B. G., Staffell, I., & Shang, J. L. (2012). Current status of hybrid, battery and fuel cell electric vehicles: from electrochemistry to market prospects. *Electrochimica Acta, 84*, 235-249.

Rahama, O. A., & Chancellor, W. J. (1994). Peak and Average Loads on Tractor Structures. *Transactions of the ASABE, 37*(6).

Schrock, M. D., Kramer, J. A., & Clark, S. J. (1985). Fuel Requirements for Field Operations in Kansas. *28*(3).

Xue, X., Cheng, K., & Cheung, N. (2008). *Selection of electric motor drives for electric vehicles.* Paper presented at the Power Engineering Conference, 2008. AUPEC'08. Australasian Universities.

VITA

Joseph William Jackson

PERSONAL:

Born Lexington, KY

EDUCATION

Bachelor of Science in Biosystems Engineering with a Minor in Chinese Studies, University of Kentucky. Graduated May 2012.

EXPERIENCE

Graduate Research Assistant: University of Kentucky Dept. of Biosystems and Agricultural Engineering, Lexington, Kentucky (2012-2015) Advisor: Dr. Joseph Dvorak